Available online at www.sciencedirect.com

ScienceDirect

Journal of Sound and Vibration 315 (2008) 197–211

JOURNAL OF SOUND AND VIBRATION

www.elsevier.com/locate/jsvi

Free vibration analysis of symmetrically laminated thin composite plates by using discrete singular convolution (DSC) approach: Algorithm and verification

Abdullah Seçgin*, A. Saide Sarıgül

Department of Mechanical Engineering, Dokuz Eylül University, 35100 Bornova, İzmir, Turkey

Received 19 July 2007; received in revised form 19 November 2007; accepted 29 January 2008
Handling Editor: C. Morfey
Available online 3 April 2008

Abstract

This study presents a detailed procedure for the implementation of a discrete singular convolution (DSC) approach to the free vibration analysis of composite plates based on classical laminated plate theory (CLPT). The approach performs a numerical solution of differential equation of motion by using a grid discretization based on distribution theory and wavelets. In the paper, firstly, computational algorithm of the DSC method is presented. Then, the accuracy of the computer code developed is verified by comparing DSC solutions with the exact results of simply supported isotropic thin beams, fully simply supported one-layer isotropic and specially orthotropic plates, and also some symmetrically laminated thin composite plates orientated to become specially orthotropic. Besides, DSC predictions for laminated composite plates with different boundary conditions and ply numbers, for which there is no analytical solution, are compared with those of several distinguished works available in the literature. It is noteworthy that DSC results completely match with the exact solutions and are in perfect agreement with those of compared studies.

1. Introduction

Laminated composites are increasingly used in various mechanical structures and industrial applications such as aircrafts, automobiles, marines, buildings and several house-hold appliances due to their, in particular, higher stiffness and higher strength-to-weight ratio compared to isotropic or wooden materials. In vibration engineering, modal parameters of a structure are primary design information, because they directly affect the forced response characteristics. Conventional methods for vibration analysis are generally based on either theoretical solutions or experimental studies. However, in general, practical problems are either too difficult or impossible to deal with by analytical methods and experiments are rather expensive. Therefore, numerical simulations and algorithms are of significant role in modern vibration analysis. The finite element method (FEM) has been commonly used in the vibration analysis of composite plates. Significant studies up to the

*Corresponding author. Tel.: +90 232 3887868; fax: +90 232 3887864.
E-mail addresses: abdullah.secgin@deu.edu.tr (A. Seçgin), saide.sarigul@deu.edu.tr (A.S. Sarıgül).

0022-460X/$ - see front matter
doi:10.1016/j.jsv.2008.01.061

1980s on the vibration analysis of laminated composite plates by the finite element method were reviewed by Reddy [1]. Reddy and Averill [2] also presented refined two-dimensional theories and computational models of laminated composite plates and reviewed the computational aspects of finite element models of these refined theories. Ritz, *p*-Ritz and Rayleigh–Ritz approaches are successfully employed in the vibration analysis of laminated plates [3–10]. The differential quadrature technique introduced by Bellman et al. [11] has been applied in the vibration analysis of both isotropic and composite plates [12–16]. Besides, several alternative techniques have been increasingly used [17–21].

In the last decade, a novel approach originally introduced by Wei [22,23] and called "discrete singular convolution (DSC)" analysis has presented a powerful technique for the numerical solution of differential equations. The solution technique of DSC is based on the theory of distribution and wavelets. The technique includes both the flexibility of local methods and the accuracy of global methods. The DSC method has been reliably used in various vibration analyses: Wei [24–26] and Wei et al. [27–29] showed that the DSC method can be effectively used in the vibration analysis of isotropic beams and plates with several uniform and non-uniform boundary conditions. Wei et al. [30] and Zhao et al. [31] proved the accuracy of the DSC method in the prediction of high natural frequencies of beams and plates. At present, these high-frequency predictions are unique results numerically obtained. Furthermore, Ng et al. [32] clearly indicated that the DSC yields more accurate predictions compared to the differential quadrature method for higher-order eigenfrequencies.

In the literature, the implementation procedure of DSC is presented rather implicitly. In this paper, the basic algorithm of the DSC approach and boundary condition implementation are clearly introduced. A computer code has been developed on the basis of the DSC for the free vibration analysis of composite plates based on classical laminated plate theory (CLPT). The accuracy of the code is verified by comparing the DSC free vibration results with the exact ones for simply supported isotropic thin beams, fully simply supported one-layer isotropic and specially orthotropic plates, and some symmetrically laminated thin composite plates orientated to become specially orthotropic. In addition, free vibrations of several laminated thin composite plates, which have no analytical solutions, are predicted by DSC for different boundary conditions and ply numbers. The results are compared with those of various published studies utilizing different methods.

2. Bending vibrations of symmetrically laminated plates based on CLPT

Time-independent differential equation of harmonic bending vibration for a symmetrically laminated thin composite plate with natural frequency ω having side lengths a and b, total thickness h, average mass density ρ_0 and Poisson rate υ can be written in Cartesian co-ordinates (x, y) in terms of flexural displacement w as follows [33]:

$$\begin{aligned} &D_{11}\frac{\partial^4 w(x,y)}{\partial x^4} + 4D_{16}\frac{\partial^4 w(x,y)}{\partial x^3 \partial y} + 2(D_{12}+2D_{66})\frac{\partial^4 w(x,y)}{\partial x^2 \partial y^2} \\ &\quad + 4D_{26}\frac{\partial^4 w(x,y)}{\partial x \partial y^3} + D_{22}\frac{\partial^4 w(x,y)}{\partial y^4} - \rho_0 h \omega^2 w(x,y) = 0. \end{aligned} \tag{1}$$

Here, D_{11}, D_{12}, D_{22} and D_{66} are the bending rigidities in the principle material directions whereas D_{16} and D_{26} are the bend-twist coupling stiffnesses. For fully simply supported (SSSS) and fully clamped (CCCC) edges, the following boundary conditions are applicable:

$$\text{For SSSS:} \quad \text{at} \quad x = 0,\ a: \quad w = 0; \quad -D_{11}\frac{\partial^2 w}{\partial x^2} - 2D_{16}\frac{\partial^2 w}{\partial x \partial y} - D_{12}\frac{\partial^2 w}{\partial y^2} = 0, \tag{2a}$$

$$\text{at} \ \ y = 0,\ b: \quad w = 0; \quad -D_{12}\frac{\partial^2 w}{\partial x^2} - 2D_{26}\frac{\partial^2 w}{\partial x \partial y} - D_{22}\frac{\partial^2 w}{\partial y^2} = 0. \tag{2b}$$

$$\text{For CCCC:} \quad \text{at} \quad x = 0,\ a: \quad w = 0; \quad \frac{\partial w}{\partial x} = 0, \tag{3a}$$

$$\text{at} \ \ y = 0,\ b: \quad w = 0; \quad \frac{\partial w}{\partial y} = 0. \tag{3b}$$

Introducing new non-dimensional parameters: $X = x/a$, $Y = y/b$, $W = w/a$, $\lambda = a/b$, $D_\gamma = (D_{11}/D_{22})$, $D_\phi = (D_{12} + 2D_{66})$, $D_\alpha = (D_{16}/D_{22})$, $D_\beta = (D_{26}/D_{22})$, Eq. (1) can be rewritten in the following form:

$$D_\gamma \frac{\partial^4 W(X,Y)}{\partial X^4} + 2\lambda^2 D_\phi \frac{\partial^4 W(X,Y)}{\partial X^2 \partial Y^2} + \lambda^4 \frac{\partial^4 W(X,Y)}{\partial Y^4} + 4\left(\lambda D_\alpha \frac{\partial^4 W(X,Y)}{\partial X^3 \partial Y} + \lambda^3 D_\beta \frac{\partial^4 W(X,Y)}{\partial X \partial Y^3}\right) - \Omega^2 W(X,Y) = 0. \tag{4}$$

Here, the natural frequency parameter is $\Omega = \omega a^2 \sqrt{\rho_0 h / D_{22}}$. For specially orthotropic plates (SOP) and isotropic plates (IP), Eq. (4) can be simplified based on the following two features:

- For the SOP: The composite is symmetrically laminated and has only plies in the 0° and 90° directions; therefore, $D_\gamma \neq D_\phi$ and $D_\alpha = D_\beta = 0$ (i.e., $D_{16} = D_{26} = 0$).
- For the isotropic plates (IP): The rigidities $D_\gamma = D_\phi = 1$ and $D_\alpha = D_\beta = 0$ (i.e., $D_{11} = D_{22} = D = Eh^3/12(1-\upsilon^2)$ and $D_{16} = D_{26} = 0$).

For fully simply supported SOP, natural frequency parameter $\Omega_{p,q}$ is analytically given by [33],

$$\Omega_{p,q} = \omega_{p,q} a^2 \sqrt{\frac{\rho_0 h}{D_{22}}} = \pi^2 \sqrt{p^4 D_\gamma + 2p^2 q^2 \lambda^2 D_\phi + q^4 \lambda^4} \quad p,q = 1,2,3,\ldots. \tag{5}$$

3. Discrete singular convolution (DSC)

3.1. Theory of the DSC

Singular convolution is defined by the theory of distributions. Let T be a distribution and $\eta(t)$ be an element of the space of test functions. Then, a singular convolution can be given by [22]

$$F(t) = (T * \eta)(t) = \int_{-\infty}^{\infty} T(t-x)\eta(x)\,\mathrm{d}x. \tag{6}$$

Here, the sign $*$ is the convolution operator, $F(t)$ is the convolution of η and T, $T(t-x)$ is the singular kernel of the convolution integral. Depending on the form of the kernel T, singular convolution can be applied to different science and engineering problems. Delta kernel is an interpolation function essential for the numerical solution of partial differential equations:

$$T(x) = \delta^n(x) \quad n = 0,1,2,\ldots \tag{7}$$

Delta kernels given in Eq. (7) are proper for use in vibration analysis. However, these kernels are singular; thus, they cannot be digitized directly in a computer. In order to avoid this problem, sequences of approximations T_α of the distributions T can be constructed such that T_α converge to T:

$$\lim_{\alpha \to \alpha_0} T_\alpha(x) \to T(x), \tag{8}$$

where α_0 is a generalized limit. With a good approximation, a Discrete Singular Convolution (DSC) can be determined as

$$F_\alpha(x) = \sum_k T_\alpha(x - x_k) f(x_k). \tag{9}$$

Here, $F_\alpha(x)$ is an approximation to $F(x)$ and $\{x_k\}$ is an approximate set of discrete points on which the DSC in Eq. (9) is well defined. $f(x)$ is used here as the test function replacing the original test function $\eta(x)$. A sequence of approximation can be improved by a regularizer in order to increase the regularity of convolution kernels. The gaussian regularizer is a typical delta regularizer and it is in the form of

$$R_\sigma(x) = \mathrm{e}^{-x^2/2\sigma^2}, \tag{10}$$

where σ is the standard deviation. Delta kernel with sampling parameter α approximately in the form

$$T_\alpha = \frac{\sin \alpha x}{\pi x}, \tag{11}$$

is known as the Shannon father wavelet (scaling function). In vibration analysis, a discretized form of Eq. (11), which is sampled by Nyquist frequency ($\alpha = \pi/\Delta$, Δ is the grid spacing) and improved by the Gaussian regularizer, can be chosen as the kernel function of the DSC [22]:

$$\delta_{\pi/\Delta,\sigma}(x - x_k) = \frac{\sin[\pi/\Delta(x - x_k)]}{\pi/\Delta(x - x_k)} \exp(-(x - x_k)^2/2\sigma^2). \tag{12}$$

Here, Δ is determined by considering the required precision of the analysis. The DSC expression in Eq. (9) can be rewritten using the Regularized Shannon Delta Kernel (RSDK) given in Eq. (12):

$$f(x) \approx \sum_{k=-\infty}^{\infty} \frac{\sin[\pi/\Delta(x - x_k)]}{\pi/\Delta(x - x_k)} \exp(-(x - x_k)^2/2\sigma^2) f(x_k). \tag{13}$$

As seen in Eq. (13), since the DSC approach is defined in an infinite region, the kernels must be bounded in a sufficient computational domain for numerical determination. This can be practically achieved by a spatial truncation of the convolution kernel. A translationally invariant symmetric truncation algorithm can be used in an efficient bandwidth $(2M+1)$ as follows:

$$f^{(n)}(x_m) \approx \sum_{k=-M}^{M} \delta^{(n)}_{\pi/\Delta,\sigma}(x_m - x_k) f(x_k). \tag{14}$$

Here, x_m is the specific central point considered and $\delta^{(n)}_{\pi/\Delta,\sigma}(x)$ is the nth derivative of $\delta(x)$ given in Eq. (12) with respect to x. As an example, the second order derivative of the RSDK can be analytically given by

$$\begin{aligned}
\delta^{(2)}_{\pi/\Delta,\sigma}(x_m - x_k) = &-\left(\frac{(\pi/\Delta)\sin[\pi/\Delta(x_m - x_k)]}{(x_m - x_k)} + 2\frac{\cos[\pi/\Delta(x_m - x_k)]}{(x_m - x_k)^2}\right) \exp(-(x_m - x_k)^2/2\sigma^2) \\
&-\left(2\frac{\cos[\pi/\Delta(x_m - x_k)]}{\sigma^2} - 2\frac{\sin[\pi/\Delta(x_m - x_k)]}{\pi/\Delta(x_m - x_k)^3}\right) \exp(-(x_m - x_k)^2/2\sigma^2) \\
&+\left(\frac{\sin[\pi/\Delta(x_m - x_k)]}{\pi/\Delta(x_m - x_k)\sigma^2} + \frac{\sin[\pi/\Delta(x_m - x_k)]}{\pi/\Delta\sigma^4}(x_m - x_k)\right) \exp(-(x_m - x_k)^2/2\sigma^2).
\end{aligned} \tag{15}$$

Specifically, the value of the kernel at $x_m = x_k$ is

$$\lim_{x_k \to x_m} \delta^{(2)}_{\pi/\Delta,\sigma}(x_m - x_k) \to \delta^{(2)}_{\pi/\Delta,\sigma}(0) = -\frac{1}{\sigma^2} - \frac{\pi^2}{3\Delta^2}. \tag{16}$$

3.2. DSC discretization of operator

In the DSC implementation to any differential equation, a linear DSC operator L having a differential part D and a function part F is written as

$$L = D + F. \tag{17}$$

It is essential to define a grid representation so that the function part of the operator is diagonal. Hence, the grid discretization is simply given by a direct interpolation:

$$F(x) \to F(x_k)\ \delta^{(0)}_{\pi/\Delta,\sigma}(x_m - x_k), \tag{18}$$

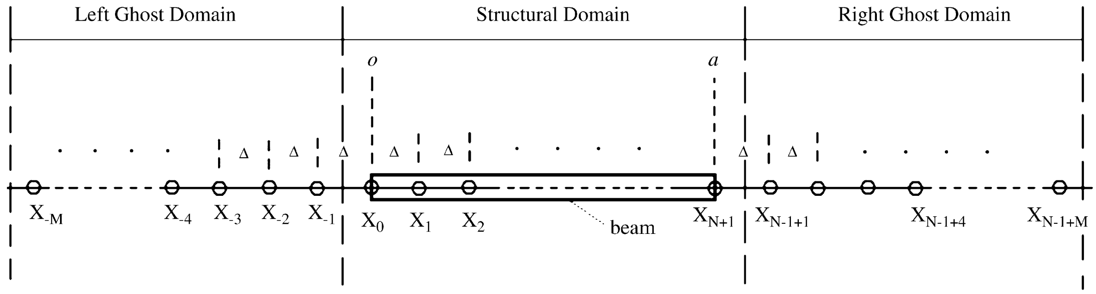

Fig. 1. Computational domain representation for a beam structure in DSC algorithm.

where $\delta^{(0)}_{\pi/\Delta,\sigma}(x_m - x_k)$ is the RSDK given in Eq. (12). The differential part of the operator on the coordinate grid is then represented by functional derivatives:

$$D = \sum_n d_n(x)\frac{d^n}{dx_n} \to \sum_n d_n(x_m)\delta^{(n)}_{\pi/\Delta,\sigma}(x_m - x_k), \tag{19}$$

where d_n is a coefficient. Finally, the linear DSC operator L can be rewritten by summing Eqs. (18) and (19);

$$L = (x_m - x_k) = \sum_n d_n(x_m)\delta^{(n)}_{\pi/\Delta,\sigma}(x_m - x_k) + F(x_k)\delta^{(0)}_{\pi/\Delta,\sigma}(x_m - x_k), \quad n \neq 0. \tag{20}$$

3.3. Grid discretization in the DSC algorithm

A thin beam having length a is illustrated in Fig. 1 as an example of DSC grid discretization. N is the number of structure points $(x_0, x_1, \ldots, x_{N-1})$ with uniform interval $\Delta = a/(N-1)$. The function derivatives on these points are approximated by a linear summation of function values on the $2M+1$ points centered at those points. Since the summation requires function values at the points outside the structural domain, M auxiliary points can be fictitiously positioned on both the left and right sides of the structural domain. For an effective algorithm, three indices, $i = 0, 1, 2, \ldots, N-1$, $k = -M, \ldots, 0, \ldots, M$ and $j = -M, \ldots, 0, \ldots, N-1+M$, may be determined with the condition that $N \geqslant M+1$. Regarding these determinations, DSC given in Eq. (14) can be rewritten as

$$W^{(n)}(x_i) \approx \sum_{k=-M}^{M} \delta^{(n)}_{\pi/\Delta,\sigma}(x_i - x_k)W(x_{i+k}). \tag{21}$$

By using translationally invariant algorithm, $k\Delta = (x_0 - x_k) = (x_1 - x_k) = \cdots = (x_{N-1} - x_k)$, a set of $(2M+1)$ coefficients for $\forall i \in \{0, 1, \ldots, N-1\}$ points is obtained:

$$\{\delta^{(n)}_{-M}, \ldots, \delta^{(n)}_0, \ldots, \delta^{(n)}_M\} = \{\delta^{(n)}_{\pi/\Delta,\sigma}(-M\Delta), \ldots, \delta^{(n)}_{\pi/\Delta,\sigma}(0), \ldots, \delta^{(n)}_{\pi/\Delta,\sigma}(M\Delta)\}. \tag{22}$$

Thus, the DSC reduces to

$$W^{(n)}(x_i) \approx \sum_{k=-M}^{M} \delta^{(n)}_{\pi/\Delta,\sigma}(k\Delta)W(x_{i+k}). \tag{23}$$

Similar representations and notations can be properly defined for other structures such as plates and acoustic enclosures.

4. Implementation of the DSC approach

4.1. Implementation of the DSC to symmetrically laminated plates

Applying linear DSC operator L, which performs the DSC approach in Eq. (23), to Eq. (4), one can obtain a discretized governing equation of symmetrically laminated composite plates in a non-dimensional form:

$$
\begin{aligned}
&D_\gamma \sum_{k=-M}^{M} \delta^{(4)}_{\pi/\Delta,\sigma}(k\Delta) W(X_{i+k}, Y) \\
&+ 2\lambda^2 D_\phi \left(\sum_{k=-M}^{M} \delta^{(2)}_{\pi/\Delta,\sigma}(k\Delta) W(X_{i+k}, Y) \sum_{k=-M}^{M} \delta^{(2)}_{\pi/\Delta,\sigma}(k\Delta) W(X, Y_{i+k}) \right) \\
&+ \lambda^4 \sum_{k=-M}^{M} \delta^{(4)}_{\pi/\Delta,\sigma}(k\Delta) W(X, Y_{i+k}) \\
&+ 4\lambda D_\alpha \left(\sum_{k=-M}^{M} \delta^{(3)}_{\pi/\Delta,\sigma}(k\Delta) W(X_{i+k}, Y) \sum_{k=-M}^{M} \delta^{(1)}_{\pi/\Delta,\sigma}(k\Delta) W(X, Y_{i+k}) \right) \\
&+ 4\lambda^3 D_\beta \left(\sum_{k=-M}^{M} \delta^{(1)}_{\pi/\Delta,\sigma}(k\Delta) W(X_{i+k}, Y) \sum_{k=-M}^{M} \delta^{(3)}_{\pi/\Delta,\sigma}(k\Delta) W(X, Y_{i+k}) \right) = \boldsymbol{\Omega}^2 \mathbf{W}(X, Y). \qquad (24)
\end{aligned}
$$

The DSC full matrix: DSC kernels in Eq. (24) can be written in a DSC matrix form as

$$
\boldsymbol{\Psi}^{(n)}_{ri,j} = \begin{cases} \delta^{(n)}_{\pi/\Delta,\sigma}((j-i)\Delta), & \text{if } -M \leqslant j-i \leqslant M, \\ 0, & \text{otherwise.} \end{cases} \qquad (25)
$$

Here, $\boldsymbol{\Psi}^{(n)}_r$ is $N \times (2M+N)$ DSC full matrix and r is the direction of differentiation ($r = x$ or y for plates).

Boundary condition implementation: The numerical scheme of the DSC is completed by implementing the boundary conditions to Eq. (24). For simply supported and clamped boundary conditions, an assumption on the relation between auxiliary points and structure points can be made by determining an arbitrary index $S = 1, \ldots, M$ and the coefficients $A_{r,\ S}$ and $B_{r,\ S}$:

For left ($r = x$) and top ($r = y$) boundaries

$$
W(r_{-S}) - W(r_0) = A_{r,S}[W(r_S) - W(r_0)]. \qquad (26)
$$

In a similar way, for right ($r = x$) and bottom ($r = y$) boundaries

$$
W(r_{N-1+S}) - W(r_{N-1}) = B_{r,S}[W(r_{N-1-S}) - W(r_{N-1})]. \qquad (27)
$$

Any auxiliary point can be written in terms of structure points using one of the relations in Eqs. (26) and (27). Then using the DSC expression in Eq. (23), one can obtain the coefficients as $A_{r,S} = B_{r,S} = -1$ for SSSS and $A_{r,S} = B_{r,S} = 1$ for CCCC plates, for each S value. As these boundary conditions are applied, a vector for a discretized plate shown in Fig. 2 is formed:

$$
\mathbf{W} = \{W_{0,0}, \ldots, W_{0,N-1}, W_{1,0}, \ldots, W_{1,N-1}, \ldots, \ldots, W_{N-1,0}, \ldots, W_{N-1,N-1}\}^{\mathrm{T}}. \qquad (28)
$$

Finally, after implementation of displacement boundary conditions $W(r_0) = W(r_{N-1}) = 0$, Eq. (24) can be reconstructed by DSC matrices as an eigenvalue equation for symmetrically laminated composite plates:

$$
\begin{aligned}
&\{D_\gamma(\boldsymbol{\Gamma}^{(4)}_x \otimes \mathbf{I}_y) + 2\lambda^2 D_\phi(\boldsymbol{\Gamma}^{(2)}_x \otimes \boldsymbol{\Gamma}^{(2)}_y) + \lambda^4(\mathbf{I}_x \otimes \boldsymbol{\Gamma}^{(4)}_y) \\
&+4\lambda D_\alpha(\boldsymbol{\Gamma}^{(3)}_x \otimes \boldsymbol{\Gamma}^{(1)}_y) + 4\lambda^3 D_\beta(\boldsymbol{\Gamma}^{(1)}_x \otimes \boldsymbol{\Gamma}^{(3)}_y)\}\mathbf{W} = \boldsymbol{\Omega}^2\mathbf{W}, \qquad (29)
\end{aligned}
$$

where $\boldsymbol{\Gamma}^{(n)}_r$is the DSC characteristic matrix, $\mathbf{I}_r$ is the identity matrix, $\boldsymbol{\Omega}$ is the diagonal natural frequency parameter matrix, $\mathbf{W}$ is the displacement vector and the symbol $\otimes$ denotes tensorial product. For square plates

$\lambda = 1$; $\mathbf{I}_x = \mathbf{I}_y$. A characteristic matrix is obtained by applying specific boundary conditions to the DSC full matrix $\boldsymbol{\Psi}_r^{(n)} N \times (2M + N)$ defined in Eq. (25). Afterwards, $\boldsymbol{\Omega}$ and $\mathbf{W}$ can be obtained from Eq. (29) using a standard solver.

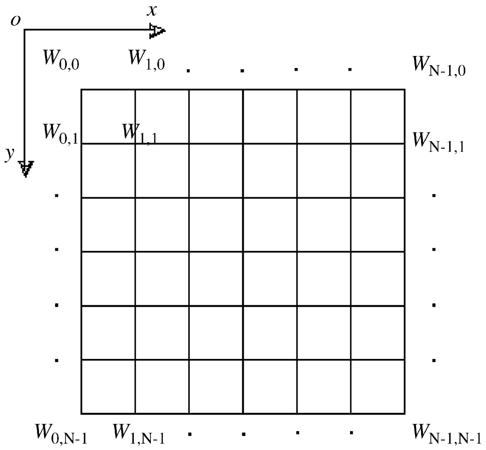

Fig. 2. DSC grid representation of a square plate (N^2: number of grid points).

Table 1
Natural frequency parameters of some simply supported structures

Isotropic beam (SS)					Isotropic square plate (SSSS)				Specially orthotropic square plate (SSSS)			
Beam length: $a = \pi$ (m) Natural frequency parameter: $\Omega = \omega\sqrt{\frac{\rho A}{EI}}$					$\lambda = 1,\ D_\gamma = D_\phi = 1,\ D_\alpha = D_\beta = 0$ Natural frequency parameter: $\Omega/\pi^2 = \omega\frac{a^2}{\pi^2}\sqrt{\frac{\rho_0 h}{D}}$				$\lambda = 1,\ D_\gamma = 10,\ D_\phi = 1,\ D_\alpha = D_\beta = 0$ Natural frequency parameter: $\Omega/\pi^2 = \omega\frac{a^2}{\pi^2}\sqrt{\frac{\rho_0 h}{D_{22}}}$			
Mode number	DSC			Exact [34]	Mode number (p, q)	DSC		Exact [33]	Mode number (p, q)	DSC		Exact [33]
	$N = 11$	$N = 21$	$N = 31$			$N = 11 \times 11$	$N = 21 \times 21$			$N = 11 \times 11$	$N = 21 \times 21$	
1	1.0050	1.0000	1.0000	1	(1,1)	2.0051	2.0000	2	(1,1)	3.6209	3.6056	3.6056
2	3.9994	4.0000	4.0000	4	(1,2)	5.0006	5.0000	5	(1,2)	5.8392	5.8310	5.8310
3	9.0095	9.0000	9.0000	9	(2,1)	5.0006	5.0000	5	(1,3)	10.4535	10.4403	10.4403
4	16.0764	16.0000	16.0000	16	(2,2)	7.9993	8.0000	8	(2,1)	12.9986	13.0000	13.0000
5	25.4813	25.0000	25.0000	25	(1,3)	10.0092	10.0000	10	(2,2)	14.4204	14.4222	14.4222
6	38.0834	36.0000	36.0000	36	(3,1)	10.0092	10.0000	10	(1,4)	17.3370	17.2627	17.2627
7	55.0104	49.0000	49.0000	49	(2,3)	13.0066	13.0000	13	(2,3)	17.6954	17.6918	17.6918
8	75.1793	64.0000	64.0000	64	(3,2)	13.0066	13.0000	13	(2,4)	23.3768	23.3238	23.3238
9	92.8390	81.0002	81.0000	81	(1,4)	17.0728	17.0000	17	(1,5)	26.6382	26.1725	26.1725
10	–	100.0022	100.0000	100	(4,1)	17.0728	17.0000	17	(3,1)	28.8224	28.7924	28.7924
11	–	121.0168	121.0000	121	(3,3)	18.0102	18.0000	18	(2,5)	29.9953	29.9666	29.9666
12	–	144.1010	144.0000	144	(2,4)	20.0628	20.0000	20	(3,2)	31.7809	31.3847	31.3847
13	–	169.4850	169.0000	169	(4,2)	20.0628	20.0000	20	(3,3)	32.4794	32.4500	32.4500
14	–	197.8500	196.0000	196	(3,4)	25.0560	25.0000	25	(1,6)	36.8558	36.7967	36.7967
15	–	230.5612	225.0000	225	(4,3)	25.0560	25.0000	25	(3,4)	39.1635	37.1214	37.1214
16	–	269.0423	256.0000	256	(1,5)	26.4671	26.0000	26	(2,6)	43.6304	41.7612	41.7612
17	–	312.5090	289.0000	289	(5,1)	26.4671	26.0000	26	(3,5)	43.7355	43.4166	43.4166
18	–	355.4072	324.0000	324	(2,5)	29.4290	29.0000	29	(1,7)	51.1619	50.0899	50.0899
19	–	387.8306	361.0000	361	(5,2)	29.4290	29.0000	29	(2,7)	52.2357	50.9215	50.9215
20	–	–	400.0000	400	(4,4)	32.0854	32.0000	32	(3,6)	54.0563	52.0000	52.0000

4.2. Convergence and comparison study

4.2.1. Verification of natural frequency parameters

In order to validate the DSC code, firstly, the natural frequency parameters of simply supported isotropic thin beams, plates (IP) and specially orthotropic thin plates (SOP) were computed. These frequency parameters are compared with the exact results in Table 1. In all analyses performed in this study, thin plates were assumed to be square. Here, natural frequency parameters of the plates were defined as Ω/π^2 for numerical facility. It can be seen from Table 1 that as the number of grid points (N) increases, the discrepancy

Table 2
Natural frequency parameters of fully clamped (CCCC) specially orthotropic plate (SOP) ($\lambda = 1$, DSC: $N = 21 \times 21$, $\Omega/\pi^2 = (\omega a^2/\pi^2)\sqrt{\rho_0 h/D_{22}}$, $D_\gamma = 10$, $D_\phi = 1$, $D_\alpha = D_\beta = 0$)

Specially orthotropic square plate (CCCC)		
Mode number (p, q)	Present: DSC	Whitney [33]
(1,1)	7.7199	7.7221
(1,2)	10.0990	10.102
(1,3)	15.0440	15.0475
(2,1)	20.1740	20.1835
(2,2)	21.7380	21.7402
(1,4)	22.4670	22.4673

Table 3
Natural frequency parameters $\beta_1 = \omega a^2\sqrt{\rho_0 h/D_{0,1}}$ of fully simply supported (SSSS) square three-ply laminates with several orientations ($\lambda = 1$, DSC: $N = 21 \times 21$)

Three-ply	Resource	Mode Sequence Number					
Ply angle		1	2	3	4	5	6
SSSS:							
(0°, 0°, 0°)	Exact [33] (CLPT: SOP)	15.171	33.248	44.387	60.682	64.457	90.145
	Present: DSC	15.171	33.248	44.387	60.682	64.457	90.145
	Dai et al. [19] (CLPT)	15.17	33.32	44.51	60.78	64.79	90.42
	Dai et al. [19] (TSDT)	15.22	33.76	44.79	61.11	66.76	91.69
	Chow et al. [8] (CLPT)	15.19	33.31	44.52	60.79	64.55	90.31
	Leissa and Narita [4] (CLPT)	15.19	33.30	44.42	60.78	64.53	90.29
(15°, −15°, 15°)	Present: DSC	15.469	34.153	43.879	60.954	66.635	91.393
	Dai et al. [19] (CLPT)	15.40	34.12	43.96	60.91	66.92	91.76
	Dai et al. [19] (TSDT)	15.45	34.54	44.25	61.36	68.68	92.99
	Chow et al. [8] (CLPT)	15.37	34.03	43.93	60.80	66.56	91.40
	Leissa and Narita [4] (CLPT)	15.43	34.09	43.80	60.85	66.67	91.40
(30°, −30°, 30°)	Present: DSC	16.058	36.060	42.743	61.757	71.849	85.780
	Dai et al. [19] (CLPT)	15.87	35.92	42.70	61.53	71.10	86.31
	Dai et al. [19] (TSDT)	15.92	36.28	43.00	62.05	73.55	87.37
	Chow et al. [8] (CLPT)	15.86	35.77	42.48	61.27	71.41	85.67
	Leissa and Narita [4] (CLPT)	15.90	35.86	42.62	61.45	71.71	85.72
(45°, −45°, 45°)	Present: DSC	16.348	37.146	42.033	62.234	77.213	80.130
	Dai et al. [19] (CLPT)	16.10	37.00	41.89	61.93	77.99	80.11
	Dai et al. [19] (TSDT)	16.15	37.33	42.20	62.45	78.96	81.55
	Chow et al. [8] (CLPT)	16.08	36.83	41.67	61.65	76.76	79.74
	Leissa and Narita [4] (CLPT)	16.14	36.93	41.81	61.85	77.04	80.00

between the DSC predictions and exact results decreases. For isotropic beams, even with low grid numbers such as $N = 11$, the first few natural frequency parameters are accurately predicted by DSC. For $N = 31$, the exact results are obtained up to the computed one ten-thousandth digits for the considered number of modes. Table 1 also shows an excellent prediction of frequency parameters for both IP and SOP by DSC, especially for $N = 21 \times 21$ grid points. In addition, for fully clamped SOP, the first six natural frequency parameters

Table 4
Natural frequency parameters $\beta_1 = \omega a^2 \sqrt{\rho_0 h / D_{0,1}}$ of fully clamped (CCCC) square three-ply laminates with several orientations ($\lambda = 1$, DSC: $N = 21 \times 21$)

Three-ply	Resource	Mode sequence number					
Ply angle		1	2	3	4	5	6
CCCC:							
(0°, 0°, 0°)	Present: DSC	29.087	50.792	67.279	85.629	87.112	118.50
	Dai et al. [19] (CLPT)	29.27	51.21	67.94	86.25	87.97	119.3
	Dai et al. [19] (TSDT)	30.02	54.68	70.41	89.36	92.58	123.6
	Chow et al. [8] (CLPT)	29.13	50.82	67.29	85.67	87.14	118.6
(15°, −15°, 15°)	Present: DSC	28.897	51.405	65.911	84.515	89.712	119.21
	Dai et al. [19] (CLPT)	29.07	51.83	66.55	85.17	90.56	120.0
	Dai et al. [19] (TSDT)	29.85	55.25	69.14	88.53	94.92	124.3
	Chow et al. [8] (CLPT)	28.92	51.43	65.92	84.55	89.76	119.3
(30°, −30°, 30°)	Present: DSC	28.522	53.124	62.683	83.821	95.158	114.13
	Dai et al. [19] (CLPT)	28.69	53.57	63.26	84.43	96.15	115.5
	Dai et al. [19] (TSDT)	29.51	56.84	66.17	87.83	100.5	118.9
	Chow et al. [8] (CLPT)	28.55	53.15	62.71	83.83	95.21	114.1
(45°, −45°, 45°)	Present: DSC	28.337	54.623	60.430	83.658	101.94	105.60
	Dai et al. [19] (CLPT)	28.50	55.11	60.94	84.25	103.2	106.7
	Dai et al. [19] (TSDT)	29.34	58.19	64.14	87.67	107.4	110.6
	Chow et al. [8] (CLPT)	28.38	54.65	60.45	83.65	102.0	105.6

Table 5
Natural frequency parameters $\beta_1 = \omega a^2 \sqrt{\rho_0 h / D_{0,1}}$ of simply supported-clamped (SCSC) square three-ply laminates with several orientations ($\lambda = 1$, DSC: $N = 21 \times 21$)

Three-ply	Resource	Mode sequence number					
Ply angle		1	2	3	4	5	6
SCSC:							
(0°, 0°, 0°)	Present: DSC	20.402	45.638	46.998	69.434	83.677	95.247
	Dai et al. [19] (CLPT)	20.48	46.04	47.15	70.12	84.54	95.85
	Dai et al. [19] (TSDT)	21.08	47.73	49.64	72.05	89.25	96.97
(15°, −15°, 15°)	Present: DSC	20.791	45.514	47.739	70.200	85.623	93.210
	Dai et al. [19] (CLPT)	20.85	45.56	48.14	70.66	86.47	94.00
	Dai et al. [19] (TSDT)	21.42	46.78	51.04	72.63	91.01	95.04
(30°, −30°, 30°)	Present: DSC	21.786	44.476	50.622	71.73	87.959	91.845
	Dai et al. [19] (CLPT)	21.84	44.42	51.03	71.89	88.96	92.82
	Dai et al. [19] (TSDT)	22.35	45.31	54.09	73.93	90.07	96.85
(45°, −45°, 45°)	Present: DSC	23.059	43.047	54.979	72.655	82.688	101.21
	Dai et al. [19] (CLPT)	23.15	43.07	55.44	72.78	83.90	102.26
	Dai et al. [19] (TSDT)	23.63	43.84	58.36	74.82	85.04	106.01

Table 6
Natural frequency parameters $\beta_1 = \omega a^2\sqrt{\rho_0 h/D_{0,1}}$ of fully simply supported (SSSS) and clamped (CCCC) square four-ply laminates with several orientations ($\lambda = 1$, DSC: $N = 21 \times 21$)

Four-ply	Resource	Mode sequence number					
Ply angle		1	2	3	4	5	6
SSSS:							
(0°, 0°, 0° , 0°)	Exact [33] (CLPT: SOP)	15.171	33.248	44.387	60.682	64.457	90.145
	Present: DSC	15.171	33.248	44.387	60.682	64.457	90.145
	Chow et al. [8] (CLPT)	15.19	33.31	44.52	60.78	64.55	90.31
	Leissa and Narita [4] (CLPT)	15.19	33.30	44.42	60.77	64.53	90.29
(15°, −15°, −15°, 15°)	Present: DSC	15.490	34.235	43.904	61.333	66.520	91.446
	Chow et al. [8] (CLPT)	15.40	34.15	43.84	61.23	66.48	91.47
	Leissa and Narita [4] (CLPT)	15.47	34.21	43.91	61.28	66.57	91.47
(30°, −30°, −30°, 30°)	Present: DSC	16.117	36.426	42.696	62.764	71.737	85.828
	Chow et al. [8] (CLPT)	15.94	36.23	42.52	62.46	71.45	85.79
	Leissa and Narita [4] (CLPT)	16.02	36.30	42.62	62.57	71.68	85.81
(45°, −45°, −45° , 45°)	Present: DSC	16.424	37.837	41.766	63.540	77.644	79.646
	Chow et al. [8] (CLPT)	16.17	37.62	41.52	63.15	77.33	79.40
	Leissa and Narita [4] (CLPT)	16.29	37.71	41.63	63.29	77.56	79.60
CCCC:							
(0°, 0°, 0° , 0°)	Present: DSC	29.087	50.792	67.279	85.629	87.112	118.50
	Chow et al. [8] (CLPT)	29.13	50.82	67.29	85.67	87.14	118.6
(15°, −15°, −15°, 15°)	Present: DSC	28.940	51.528	65.959	85.07	89.53	119.88
	Chow et al. [8] (CLPT)	28.98	51.56	65.97	85.11	89.57	119.9
(30°, −30°, −30°, 30°)	Present: DSC	28.648	53.597	62.720	85.093	95.088	114.26
	Chow et al. [8] (CLPT)	28.69	53.62	62.74	85.09	95.15	114.3
(45°, −45°, −45° , 45°)	Present: DSC	28.503	55.534	60.197	85.254	102.52	105.18
	Chow et al. [8] (CLPT)	28.53	55.56	60.22	85.25	102.6	105.2

Table 7
Natural frequency parameters $\beta_1 = \omega a^2\sqrt{\rho_0 h/D_{0,1}}$ of fully simply supported (SSSS) and clamped (CCCC) square five-ply laminates with several orientations ($\lambda = 1$, DSC: $N = 21 \times 21$)

Five-ply	Resource	Mode sequence number					
Ply angle		1	2	3	4	5	6
SSSS:							
(0°, 0°, 0° , 0° ,0°)	Exact [33] (CLPT: SOP)	15.171	33.248	44.387	60.682	64.457	90.145
	Present: DSC	15.171	33.248	44.387	60.682	64.457	90.145
	Chow et al. [8] (CLPT)	15.19	33.31	44.52	60.78	64.55	90.31
	Leissa and Narita [4] (CLPT)	15.19	33.30	44.42	60.77	64.53	90.29
(15°, −15°, 15°, −15°, 15°)	Present: DSC	15.506	34.296	43.922	61.630	66.419	91.485
	Chow et al. [8] (CLPT)	15.46	34.24	43.88	61.59	66.42	91.52
	Leissa and Narita [4] (CLPT)	15.50	34.30	43.93	61.62	66.48	91.51
(30°, −30°, 30°, −30°, 30°)	Present: DSC	16.161	36.705	42.652	63.561	71.598	85.864
	Chow et al. [8] (CLPT)	15.98	36.58	42.53	63.37	71.43	85.86
	Leissa and Narita [4] (CLPT)	16.10	36.64	42.62	63.45	71.60	85.88
(45°, −45°, 45°, −45°, 45°)	Present: DSC	16.480	38.436	41.478	64.563	77.958	79.223
	Chow et al. [8] (CLPT)	16.29	38.30	41.32	64.35	77.77	79.09
	Leissa and Narita [4] (CLPT)	16.40	38.37	41.40	64.41	77.94	79.23

Table 7 (*continued*)

Five-ply	Resource	Mode sequence number					
Ply angle		1	2	3	4	5	6
CCCC:							
(0°, 0°, 0° , 0° ,0°)	Present: DSC	29.087	50.792	67.279	85.629	87.112	118.50
	Chow et al. [8] (CLPT)	29.13	50.82	67.29	85.67	87.14	118.6
(15°, −15°, 15°, −15°, 15°)	Present: DSC	28.972	51.620	65.995	85.527	89.350	120.40
	Chow et al. [8] (CLPT)	29.00	51.65	66.01	85.55	89.40	120.5
(30°, −30°, 30°, −30°, 30°)	Present: DSC	28.740	53.951	62.741	86.097	94.968	114.35
	Chow et al. [8] (CLPT)	28.78	53.98	62.76	86.09	95.04	114.4
(45°, −45°, 45°, −45°, 45°)	Present: DSC	28.624	56.308	59.917	86.486	102.95	104.81
	Chow et al. [8] (CLPT)	28.68	56.34	59.94	86.48	103.0	104.9

Table 8
Natural frequency parameters $\beta_2 = \omega a^2/\pi^2\sqrt{\rho_0 h/D_{0,2}}$ of fully simply supported (SSSS) and fully clamped (CCCC) square three-ply laminates with (0°, 90°, 0°) orientation ($\lambda = 1$, DSC: $N = 21 \times 21$)

Three-ply (0°, 90°, 0°)	Mode sequence number							
Resource	1	2	3	4	5	6	7	8
SSSS:								
Exact [33] (CLPT: SOP)	6.6254	9.4473	16.2056	25.1181	26.5017	26.6585	30.3175	37.7892
Present: DSC	6.6254	9.4473	16.2056	25.1181	26.5017	26.6585	30.3175	37.7892
Liew [6]	6.6252	9.4470	16.2051	25.1146	26.4982	26.6572	30.3139	37.7854
Ferreira and Fasshauer [20]	6.6180	9.4368	16.2192	25.1131	26.4938	26.6667	30.2983	37.7850
Lanhe et al. [16]	6.632	9.464	16.364	25.325	26.886	–	–	–
CCCC:								
Present: DSC	14.6692	17.6191	24.5235	35.5614	39.1818	40.7945	44.8174	50.3613
Liew [6]	14.6655	17.6138	24.5114	35.5318	39.1572	40.7685	44.7865	50.3226
Ferreira and Fasshauer [20]	14.8138	17.6181	24.1145	36.0900	39.0170	40.8323	44.9457	49.0715
Lanhe et al. [16]	14.674	17.668	24.594	35.897	39.625	–	–	–

obtained by the DSC and by an approximate formula given by Whitney [33] are compared in Table 2. As seen from Table 2, the result couples are very close to each other.

Secondly, the natural frequency parameters of three-ply laminates predicted by the DSC approach are compared with those of some selected studies [4,8,19]: Leissa and Narita [4] use the Ritz method, Chow et al. [8] utilize the Rayleigh–Ritz approach whereas Dai et al. [19] introduce a mesh-free technique; and present results from classical laminated plate theory (CLPT) and Reddy's third-order shear deformation theory (TSDT). In this comparison, the natural frequency parameter is determined as $\beta_1 = \omega a^2\sqrt{\rho_0 h/D_{0,1}}$by means of an arbitrary rigidity expression (i.e., $D_{0,1} = E_1 h^3/(1 - \nu_{12}\nu_{21})$). The following plate parameters are adapted to the comparison: $E_1/E_2 = 2.45$, $G_{12} = 0.48E_2$, $\upsilon_{12} = 0.23$, $\upsilon_{21} = 0.0939$, $\rho = 8000\,\mathrm{kg\,m^{-3}}$, $h = 0.06\,\mathrm{m}$, $h/a = 0.006$ (i.e., a typical thin plate). Here, E_i, $G_{i,j}$ and $\nu_{i,j}$ are elasticity modulus, shear modulus and Poisson's ratio, respectively. Subscripts i and j denote principal fiber directions. Table 3 gives frequency parameters of the plates with fully simply supported (SSSS), Table 4 with fully clamped (CCCC) and Table 5 with simply supported-clamped (SCSC) boundary conditions. Tabulated frequency parameters computed by the DSC are in good agreement with those of the compared studies.

Thirdly, the natural frequency parameters of four- and five-ply laminates are compared in Tables 6 and 7, respectively, with those of Leissa and Narita [4] and Chow et al. [8]. Here, the frequency parameter and plate parameters are the same as given in the second case. These DSC predictions also exhibit very good agreement with the compared results.

Finally, another comparison is given for (0°, 90°, 0°) fiber orientation. Here the reference studies are by Liew [6] using the *p*-Ritz approach, Ferreira and Fasshauer [20] introducing the radial basis function-pseudospectral approach and Lanhe et al. [16] utilizing the moving least squares-differential quadrature method. In this case, the natural frequency parameter is determined as $\beta_2 = \omega a^2/\pi^2\sqrt{\rho_0 h/D_{0,2}}$ by means of another arbitrary rigidity expression (i.e., $D_{0,2} = E_2 h^3/(1 - v_{12}v_{21})$). The plate parameters are $E_1/E_2 = 40$, $G_{12} = 0.6E_2$, $\upsilon_{12} = 0.25$, $\upsilon_{21} = 0.00625$, $h = 0.001\,\mathrm{m}$, $h/a = 0.001$. DSC solutions for fully simply supported (SSSS) and fully clamped (CCCC) plates are very close to the compared results as shown in Table 8.

Moreover, as seen from Tables 3, 6, 7 and 8, in the given number of digits, DSC predictions completely match with the exact results of simply supported laminates orientated to become specially orthotropic. This implies the superiority of the DSC compared to the other techniques. It is known that the thin plate theory is not very accurate in the vibration analysis of laminated plates. However, the presented DSC results based on CLPT are sensitive because of the sufficiently small thickness-to-length ratio of the considered plates, as seen in the same predictions of exact CLPT and SOP cases.

4.2.2. *Verification of mode shapes*

Fig. 3 displays well-known first four mode shapes of a simply supported beam obtained by the DSC approach using $N = 31$ grid points. In Fig. 4, the first four mode shapes of SOP by DSC are given together with symbolic nodal line representation by Whitney [33]. For the verification of mode shapes of laminated plates, five-ply fully simply supported composite plates having $\{\theta, -\theta, \theta, -\theta, \theta\}$ sequence with four orientation angles $\theta = 0°, 15°, 30°, 45°$ are considered. In Fig. 5, the first eight mode shapes ($n = 1, 2, \ldots, 8$) corresponding to the first eight natural frequency parameters ($\beta_1 = \omega a^2\sqrt{\rho_0 h/D_{0,1}}$) tabulated in Table 9 are compared with those of Chow et al. [8]. Here the material properties are $E_1/E_2 = 15.4$, $G_{12} = 0.79E_2$, $\upsilon_{12} = 0.3$, $\upsilon_{21} = 0.0195$. These consistent mode shapes simply verify the accuracy of the DSC.

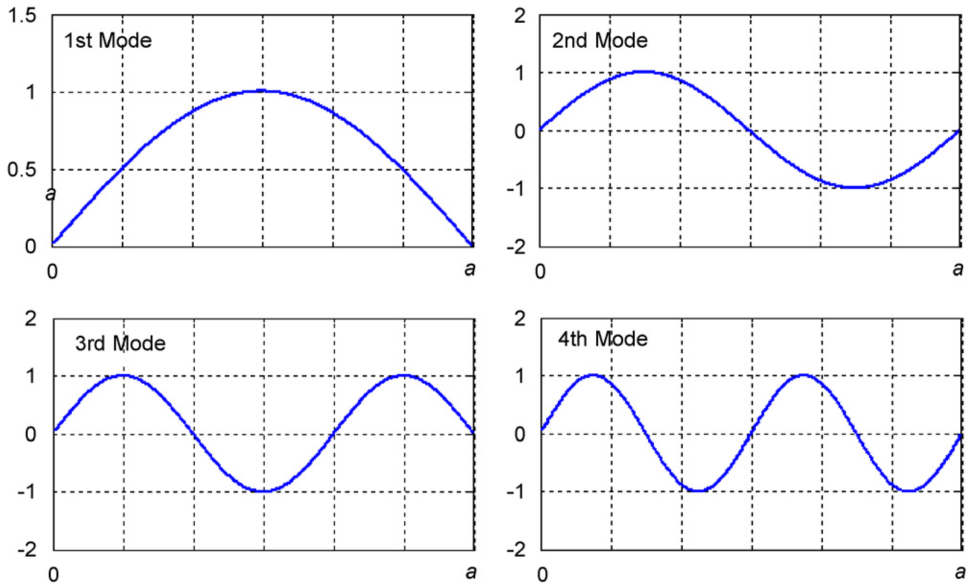

Fig. 3. The first four mode shapes of simply supported isotropic thin beam predicted by DSC ($N = 31$).

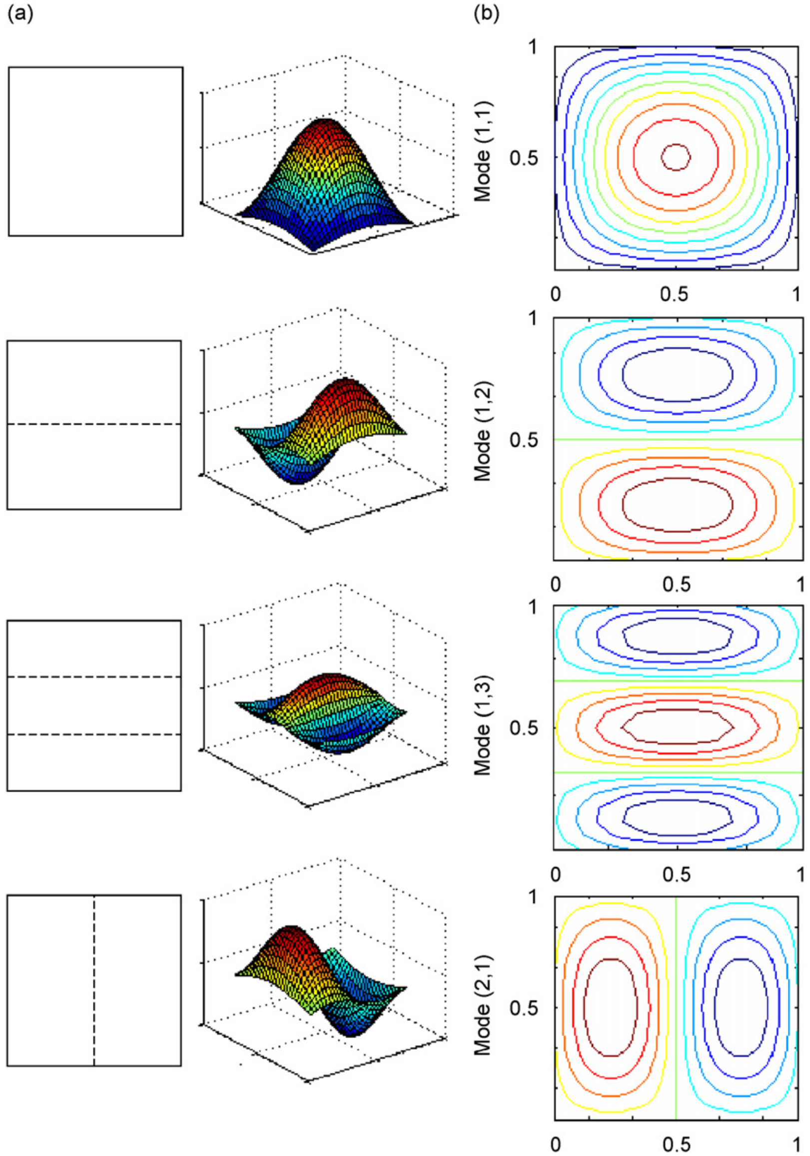

Fig. 4. The first four mode shapes of simply supported specially orthotropic thin plate: (a) Exact [33], (b) DSC ($N = 21 \times 21$).

5. Conclusions

Thin plates made of composite materials present many advantages in the use of several industrial applications. Although a number of commercial codes based on conventional methods are used in the vibration analysis of composite structural elements, researchers have been working to develop more accurate, more effective, easy to use, operational frequency-independent new approaches. In this regard, this study proves the applicability of the DSC approach to the free vibration analysis of composite plates. The paper provides open algorithms of the DSC together with some key points in the implementation procedure. Very accurate predictions have been obtained for both isotropic and orthotropic plates by using small grid numbers, leading to very small computation time and memory. Moreover, very good agreement between the DSC and other approaches used in the selected references has been obtained for symmetrically laminated composite plates. Perfect match between the DSC and exact solutions promises that the DSC approach can be reliably used in the vibration analysis of composite plates, which have no analytical solutions.

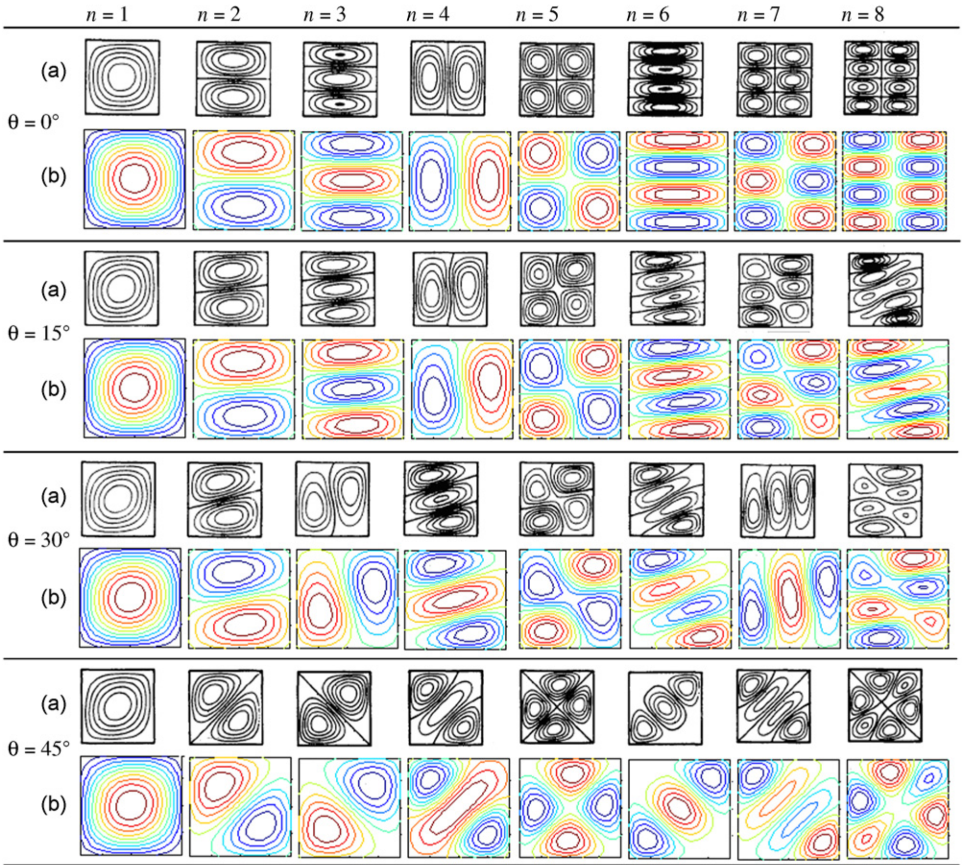

Fig. 5. The first eight mode shapes of simply supported five-ply composite plates: (a) Chow et al. [8], (b) DSC ($N = 21 \times 21$) (n: mode sequence number, θ: orientation angle).

Table 9
Natural frequency parameters $\beta_1 = \omega a^2 \sqrt{\rho_0 h / D_{0,1}}$ corresponding to the first eight mode shapes of fully simply supported (SSSS) square five-ply laminates with several orientations ($\lambda = 1$, DSC: $N = 21 \times 21$)

Five-ply	Resource	Mode sequence number							
Ply angle		1	2	3	4	5	6	7	8
(0°, 0°, 0° , 0° , 0°)	Present DSC	11.29	17.13	28.68	40.74	45.15	45.78	54.06	68.14
	Chow et al. [8]	11.30	17.13	28.70	40.77	45.18	46.23	54.98	69.64
(15°, −15°, 15°, −15°, 15°)	Present DSC	12.01	20.07	33.38	39.78	47.80	51.75	61.44	74.27
	Chow et al. [8]	11.82	19.76	32.93	39.53	47.42	52.73	61.11	74.08
(30°, −30°, 30°, −30°, 30°)	Present DSC	13.40	25.83	37.41	43.60	53.80	66.50	76.06	77.23
	Chow et al. [8]	12.98	25.21	36.97	42.65	52.83	66.48	75.76	77.65
(45°, −45°, 45°, −45°, 45°)	Present DSC	14.06	29.38	35.36	49.94	60.22	66.19	75.31	89.17
	Chow et al. [8]	13.61	28.75	34.68	48.90	59.25	65.34	74.28	88.86

References

[1] J.N. Reddy, A review of the literature on finite-element modeling of laminated composite plates, *The Shock and Vibration Digest* 17 (4) (1985) 3–8.

[2] J.N. Reddy, R.C. Averill, Advances in the modeling of laminated plates, *Computing Systems in Engineering* 2 (5) (1991) 541–555.

[3] R. Hearmon, The frequency of flexural vibrations of rectangular orthotropic plates with clamped or simply supported edges, *Journal of Applied Mechanics* 26 (1959) 537–542.

[4] A.W. Leissa, Y. Narita, Vibration studies for simply supported symmetrically laminated rectangular plates, *Composite Structures* 12 (1989) 113–132.

[5] K.M. Liew, C.W. Lim, Vibratory characteristics of general laminates, I: symmetric trapezoids, *Journal of Sound and Vibration* 183 (4) (1995) 615–642.

[6] K.M. Liew, Solving the vibration of thick symmetric laminates by Reissner/Mindlin plate theory and the *p*-Ritz method, *Journal of Sound and Vibration* 198 (3) (1996) 343–360.

[7] K.M. Liew, K.Y. Lam, S.T. Chow, Study on flexural vibration of triangular composite plates influenced by fibre orientation, *Composite Structures* 13 (2) (1989) 123–132.

[8] S.T. Chow, K.M. Liew, K.Y. Lam, Transverse vibration of symmetrically laminated rectangular composite plates, *Composite Structures* 20 (4) (1992) 213–226.

[9] K.C. Hung, K.M. Liew, K.M. Lim, S.L. Leong, Boundary beam characteristics orthonormal polynomials in energy approach for vibration of symmetric laminates-I: classical boundary conditions, *Composite Structures* 26 (1993) 167–184.

[10] P. Venini, C. Mariani, Free vibrations of uncertain composite plates via stochastic Rayleigh–Ritz approach, *Computers and Structures* 64 (1) (1997) 407–423.

[11] R. Bellman, B.G. Kashef, J. Casti, Differential quadrature: a technique for the rapid solution of nonlinear partial differential equations, *Journal of Computational Physics* 10 (1) (1972) 40–52.

[12] C.W. Bert, M. Malik, The differential quadrature method for irregular domains and application to plate vibration, *International Journal of Mechanical Sciences* 38 (6) (1996) 589–606.

[13] H. Zeng, C.W. Bert, A differential quadrature analysis of vibration for rectangular stiffened plates, *Journal of Sound and Vibration* 241 (2) (2001) 247–252.

[14] J.C. Zhang, T.Y. Ng, K.M. Liew, Three-dimensional theory of elasticity for free vibration analysis of composite laminates via layerwise differential quadrature modelling, *International Journal for Numerical Methods in Engineering* 57 (2003) 1819–1844.

[15] K.M. Liew, Y.Q. Huang, J.N. Reddy, Vibration analysis of symmetrically laminated plates based on FSDT using the moving least squares differential quadrature method, *Computer Methods in Applied Mechanics and Engineering* 192 (19) (2003) 2203–2222.

[16] W. Lanhe, L. Hua, W. Daobin, Vibration analysis of generally laminated composite plates by the moving least squares differential quadrature method, *Composite Structures* 68 (2005) 319–330.

[17] K.M. Liew, J. Wang, T.Y. Ng, M.J. Tan, Free vibration and buckling analyses of shear-deformable plates based on FSDT mesh-free method, *Journal of Sound and Vibration* 276 (2004) 997–1017.

[18] J. Wang, K.M. Liew, M.J. Tan, S. Rajendran, Analysis of rectangular laminated composite plates via FSDT meshless method, *International Journal of Mechanical Sciences* 44 (7) (2002) 1275–1293.

[19] K.Y. Dai, G.R. Liu, K.M. Lim, X.L. Chen, A mesh-free method for static and free vibration analysis of shear deformable laminated composite plates, *Journal of Sound and Vibration* 269 (2004) 633–652.

[20] A.J.M. Ferreira, G.E. Fasshauer, Analysis of natural frequencies of composite plates by an RBF-pseudospectral method, *Composite Structures* 79 (2007) 202–210.

[21] L. Liu, L.P. Chua, D.N. Ghista, Mesh-free radial basis function method for static, free vibration and buckling analysis of shear deformable composite laminates, *Composite Structures* 78 (2007) 58–69.

[22] G.W. Wei, Discrete singular convolution for the solution of Fokker–Plank equation, *Journal of Chemical Physics* 110 (18) (1999) 8930–8942.

[23] G.W. Wei, Discrete singular convolution for the sine-Gordon equation, *Physica D* 137 (2000) 247–259.

[24] G.W. Wei, Discrete singular convolution for beam analysis, *Engineering Structures* 23 (2001) 1045–1053.

[25] G.W. Wei, Vibration analysis by using discrete singular convolution, *Journal of Sound and Vibration* 244 (3) (2001) 535–553.

[26] G.W. Wei, A new algorithm for solving some mechanical problems, *Computational Methods in Applied Mechanics and Engineering* 190 (2001) 2017–2030.

[27] G.W. Wei, Y.B. Zhao, Y. Xiang, The determination of natural frequencies of rectangular plates with mixed boundary conditions by discrete singular convolution, *International Journal of Mechanical Sciences* 43 (2001) 1731–1746.

[28] G.W. Wei, Y.B. Zhao, Y. Xiang, Discrete singular convolution and its application to the analysis of plates with internal supports. Part 1: theory and algorithm, *International Journal of Numerical Methods in Engineering* 55 (2002) 913–946.

[29] Y.B. Zhao, G.W. Wei, DSC analysis of rectangular plates with non-uniform boundary conditions, *Journal of Sound and Vibration* 255 (2) (2002) 203–228.

[30] G.W. Wei, Y.B. Zhao, Y. Xiang, A novel approach for the analysis of high-frequency vibrations, *Journal of Sound and Vibration* 257 (2) (2002) 207–246.

[31] Y.B. Zhao, G.W. Wei, Y. Xiang, Discrete singular convolution for the prediction of high frequency vibration of plates, *International Journal for Solids and Structures* 39 (2002) 65–88.

[32] C.H.W. Ng, Y.B. Zhao, G.W. Wei, Comparison of discrete singular convolution and generalized differential quadrature for the vibration analysis of rectangular plates, *Computer Methods in Applied Mechanics and Engineering* 193 (2004) 2483–2506.

[33] J.M. Whitney, *Structural Analysis of Laminated Anisotropic Plates*, Technomic Publishing Company Inc., Pennsylvania, 1987.

[34] S. Timoshenko, D. Young, W. Weaver, *Vibration Problems in Engineering*, Wiley, New York, 1971.